Effects of silver-graphene oxide on seed germination and early growth of crop species

Min-Ji Kim[1], Woong Kim[1], Haegeun Chung[2*]

[1]Department of Materials Science and Engineering, Korea University, Seoul 02473, Republic of Korea

[2]Department of Environmental Engineering, Konkuk University, Seoul, 05029, Republic of Korea

Corresponding Author:

Haegeun Chung[2]

Konkuk University, 120, Neungdong-ro, Gwangjin-gu, Seoul, 05029, Republic of Korea

Email address: hchung@konkuk.ac.kr

Abstract

Due to its excellent material properties, silver-graphene oxide (Ag-GO) is being studied for diverse applications, such as antimicrobial agents, catalysts, and absorbents. Such use of Ag-GO may lead to its release into terrestrial ecosystems, but little is known about the impact of Ag-GO on plants. In the present study, we determined the effects of Ag-GO on seed germination and early growth of crop species by analyzing the germination rate, growth of roots and shoots, hydrogen peroxide (H_2O_2) accumulation, and the uptake of Ag in alfalfa, radish, and cucumber treated with 0.2 to 1.6 mg mL^{-1} of Ag-GO. Ag-GO treatment increased the shoot growth of radish at 0.2 to 1.6 mg mL^{-1} but decreased that of cucumber at 0.8 mg mL^{-1}. In addition, Ag-GO enhanced the root elongation of radish at 0.2 mg mL^{-1} but inhibited that of alfalfa at 0.2, 0.8, and 1.6 mg mL^{-1}. Ag-GO treatment induced H_2O_2 production in alfalfa, radish, and cucumber in a concentration-dependent manner. Larger amounts of Ag accumulated in the seedlings as the concentration of Ag-GO increased, and such accumulation suggests that Ag may be transferred to higher trophic levels when plants are exposed to Ag-GO in ecosystems. Our study can, thus, serve as an important basis for setting guidelines for the release of nanomaterials into the environment.

Introduction

With the rapid progress of nanotechnology in recent years, nanomaterials are being used in many products, including cosmetics, agrochemicals, and biochemical sensors (Alivisatos, 2004; Nair et al., 2010; Fleming and Ulijn, 2014; Yang et al., 2019). One of the most widely used nanomaterials for commercial products is silver nanoparticle (Ag NP), owing to their superb material characteristics, including a high antibacterial activity and unique surface plasmon resonance (Ahamed, Mohamad & Siddiqui, 2010; Vance et al., 2015). However, Ag NPs can be easily aggregated; therefore, nanocomposites have been formed with carbon materials such as graphene oxide (GO) and photocatalytic materials as supporting materials to maintain the stability of Ag NPs. As the result of the oxidation of graphite, GO with sp^2-bonded carbon atoms has many oxygen functional groups, allowing Ag NPs to be formed easily on a sheet of GO. The formation of Ag NPs on a GO sheet not only prevents the agglomeration of Ag NPs, but also enhances their material properties, such as their antibacterial activity and electronic and magnetic properties (Xu et al., 2011; Li et al., 2013). Due to its excellent properties, Ag-GO is increasingly being studied for many applications, e.g., as an antibacterial agent for water disinfection, application on membranes for antifouling, catalysts, and electrochemical biosensors (Bao, Zhang & Qi, 2011; Ko et al., 2018; Naeem et al., 2019; Zhao et al., 2019). Thus, the potential of Ag-GO for application in diverse fields warrants investigation into its environmental impacts.

In addition to the abovementioned applications, Ag-GO with high antimicrobial activity has been investigated as a novel antimicrobial agent for the control of crop diseases (Ocsoy et al., 2013; Chen et al., 2016; Liang, Yang & Cui, 2017). Ag-GO has been shown to have a higher antibacterial activity against *Xanthomonas perforans*, a tomato bacterial spot pathogen, than GO

82   or Ag NPs alone. Ag-GO deformed the bacterial structure and destroyed the cell membrane by
83   wrapping the *X. perforans* cell, while exerting no phytotoxicity against tomato leaves (Ocsoy et
84   al., 2013). Similarly, 2.5 µg mL^{-1} of Ag-GO had antibacterial activity against bacterial leaf blight
85   of rice caused by *Xanthomonas oryzae* pv. *oryzae (Xoo)*. Ag-GO damaged the structure of the
86   *Xoo* cell wall and membrane, and caused leakage of the cell contents (Liang, Yang & Cui, 2017).
87   In addition, Ag-GO deformed the structure of hyphae and induced reactive oxygen species
88   (ROS) in *Fusarium graminearum,* which cause leaf spot disease (Chen et al., 2016). Hence, the
89   antimicrobial activity of Ag-GO makes it a potential agent for controlling crop diseases. Given
90   the high potential for the application of Ag-GO in various fields, it is important to determine the
91   influence of Ag-GO on terrestrial ecosystems, especially on plants that play a central role in
92   ecosystems as a primary producer.
93
94   Several studies have demonstrated the effects of Ag NPs on seed germination and plant growth
95   (Barrena et al., 2009; El-Temsah and Joner, 2013; Rui et al., 2017; Yang et al., 2018). Treatment
96   with 0.1 mg mL^{-1} of Ag NPs inhibited the root elongation of cucumber by 15%, but it had no
97   significant effect on the root elongation of lettuce (Barrena et al., 2009). In another study,
98   treatment with Ag NPs that are 5 nm in diameter reduced the shoot length of flax and barley at
99   10 mg L^{-1}, and that of ryegrass at 10, 20, and 100 mg L^{-1}. For Ag NPs that are 20 nm in diameter,
100 the shoot growth of all three plants was inhibited at 20 mg L^{-1}; thus, the inhibitory effect of Ag
101 NPs was not size-dependent (El-Temsah and Joner, 2013). In addition, inhibited growth was
102 observed in wheat and peanuts grown in soils amended with Ag NPs (Rui et al., 2017; Yang et
103 al., 2018).
104
105 Other reports have shown both positive and negative effects of graphene on plants (Begum,
106 Ikhtiari & Fugetsu, 2011; Zhang et al., 2015; Jiao et al., 2016). Treatment with 2 mg mL^{-1} of
107 graphene for 20 days significantly reduced the growth and biomass of cabbage, red spinach, and
108 tomato seedlings. Furthermore, graphene caused oxidative stress and membrane leakage in these
109 species. However, lettuce treated at this dosage of graphene showed no significant difference in
110 plant growth or H$_2$O$_2$ production (Begum, Ikhtiari & Fugetsu, 2011). In contrast, another study
111 demonstrated that graphene at 40 µg mL^{-1} positively affected seed germination and seedling
112 growth of tomato. More specifically, treatment with graphene increased the stem and root
113 lengths and total fresh weight of tomato seedlings because graphene could penetrate seed husks,
114 resulting in the facilitation of water uptake (Zhang et al., 2015). In another study, treatment with
115 20 mg L^{-1} GO decreased the root length of tobacco compared with that of the control on day 20,
116 but it enhanced the root length of tobacco by two to three times more than that of the control
117 after 35 days. Moreover, GO increased the activity of peroxidase (POD), superoxide dismutase
118 (SOD), and catalase (CAT) and decreased the malondialdehyde (MDA) content in tobacco
119 seedlings (Jiao et al., 2016).
120

121   Despite the reports on the effects of Ag NPs and GO on various plant species, few studies have
122   been conducted to investigate the impact of Ag-GO on plants. In the present study, we
123   determined the effects of Ag-GO on seed germination and early growth of three plant species,
124   alfalfa, radish, and cucumber. Alfalfa, used as fodder, plays an important role in agricultural
125   ecosystems by fixing nitrogen. Radish and cucumber are vegetable crops that have been
126   previously used to investigate the effects of nanomaterials (Wierzbicka and Obidzińska, 1998;
127   Migliore, Cozzolino & Fiori, 2003). We examined changes in the germination rate and shoot and
128   root lengths to investigate the potential effects of Ag-GO on germination and seedling growth
129   and measured the H_2O_2 content to confirm the oxidative stress due to ROS. In addition, the Ag
130   content in the seedlings of the three species was measured to determine the uptake of Ag upon
131   Ag-GO treatment.
132

133   ## Materials & Methods
134   **Synthesis and characterization of Ag-GO**
135   GO was prepared using a modification of Hummers' method described elsewhere (Hummers and
136   Offeman, 1958; Chung et al., 2015), and Ag-GO was synthesized by the glucose reduction
137   method (Tang et al., 2013; Kim et al., 2018). Briefly, 50 mL of an aqueous GO solution (0.5 mg
138   mL^{-1}) was ultrasonicated for 1 h using a bar sonicator (VC 750 ultrasonic processor, Sonic &
139   Materials Inc., USA). The GO solution was mixed uniformly with 10 mL polyvinylpyrrolidone
140   (PVP) solution (4 mg mL^{-1}, average molecular weight ~29,000, Sigma-Aldrich) and 800 mg
141   glucose (Sigma-Aldrich), and the solution was heated at 45 °C. Subsequently, silver-ammonium
142   hydroxide solution (10 mL) was added and the solution was held at 45 °C for 7 min. The mixture
143   was centrifuged at 12,298 ×g for 10 min and the supernatant was decanted; the remaining pellet
144   was washed several times with deionized (DI) water to remove excess ions and dried at 80 °C.
145

146   The microscopic morphology of Ag-GO was observed by transmission electron microscopy
147   (Tecnai 20, FEI, USA). Absorption spectra were recorded using a UV-VIS spectrophotometer
148   (Varian Cary 50, Cary, USA). Raman spectroscopy was conducted using a LabRAM ARAMIS
149   IR2 (Horiba, Japan) to analyze the defects and strain in Ag-GO and GO. X-ray photoelectron
150   spectroscopy (XPS) spectra were measured with an automated XPS Microprobe (PHI 5000
151   Versa Probe, ULVAC-PHI, Japan) to compare the surface bonding before and after deposition of
152   Ag NPs on the GO sheet; the ratio of Ag to GO was calculated through XPS.
153

154   **Seed exposure**
155   Three plant species, alfalfa (*Medicago sativa* L.), radish (*Raphanus sativus.* L.), and cucumber
156   (*Cucumis sativus* L.), were used in our study, and the seeds of these plants which were stored
157   after harvest were purchased from Danong Inc. Korea. Before exposure to the nanomaterials,
158   seeds were soaked in a 10% sodium hypochlorite solution for 10 min to sterilize them and rinsed
159   with DI water three times (US Environmental Protection Agency, 2012). Ten sterilized seeds
160   were transferred onto filter paper placed in a 100 × 15 mm Petri dish containing 5 mL of Ag-GO

161   suspension at different concentrations (0, 0.2, 0.4, 0.8, and 1.6 mg mL^{-1}). The different
162   concentrations were prepared by diluting the stock Ag-GO suspension of 1.6 mg mL^{-1}.
163   Additionally, 1.6 mg mL^{-1} of GO and Ag NPs were applied to seeds to compare their effects to
164   those of Ag-GO. Ag NPs (Sigma-Aldrich) were stabilized using polyvinylpyrrolidone (PVP) and
165   their diameter was 70.2 ± 4.9 nm (Yasur and Rani, 2013). Petri dishes were sealed with parafilm
166   and incubated at 25 ºC in the dark for seven days. Four replicates of each treatment were
167   analyzed, for a total of 40 seeds per test species. During incubation, the germination percentage
168   was determined every two days by counting the number of germinated seeds that had roots
169   longer than 2 mm; the shoot and root lengths were measured at the end of the incubation period
170   using a ruler.
171
172   **Analysis of H_2O_2 in seedlings**
173   The Amplex® red hydrogen peroxide/peroxidase assay kit (Invitrogen™, USA) was used for the
174   determination of H_2O_2 on day 7 at the end of the experiment. Seedlings were washed with DI
175   water to remove nanomaterials on the surface of the seedlings. Adhering moisture was removed
176   from the seedlings before grinding them in liquid nitrogen using a mortar and pestle. Fifty
177   milligrams of tissue powder were resuspended in 250 μL of cold phosphate buffer (20 mM
178   K_2HPO_4, pH 6.5). After centrifugation at 4 °C, 50 μL of supernatant was incubated with 0.2 U
179   mL^{-1} horseradish peroxidase and 100 μM Amplex red reagent (10-acetyl-3,7-
180   dihydrophenoxazine) at room temperature in the dark for 30 min. Subsequently, the fluorescence
181   was measured with a Synergy HT multi-mode microplate reader (Biotek, USA) (excitation at
182   530 nm and emission at 590 nm).
183
184   **Quantification of silver content in fresh seedlings**
185   Ag content in seedlings was quantified on day 7, at the end of the experiment, following the
186   method described by Geisler-Lee et al. (2012) with modifications. Seedlings of the three species
187   were washed with DI water and their fresh weight was measured. Seedlings were fully digested
188   using a mixture of 2 mL of HNO_3 used for trace-metal analysis (70%, Sigma-Aldrich) and 1 mL
189   Co standard solution (1000 mg mL^{-1} in nitric acid, Sigma-Aldrich) heated at 120 ºC for 30 min.
190   After the solution cooled down, 2 mL of H_2O_2 used for trace analysis (H_2O_2, ~30% w/w, Sigma-
191   Aldrich) was added and the mixture was heated at 120 ºC for 30 min. The digested samples were
192   diluted with DI water to 20 mL and filtered using a 0.22-μm polyvinylidene fluoride (PVDF)
193   syringe filter. Each diluted sample was analyzed using an inductively coupled plasma-optical
194   emission spectrometer (ICP-OES, iCAP6300 Duo, Thermo Scientific, USA).
195
196   **Statistical analyses**
197   Statistical analyses were carried out using SAS® version 9.4 (SAS Inc., USA) to test the effects
198   of Ag-GO, Ag, and GO on seed germination. One-way analyses of variance (ANOVA) were
199   employed to determine the effect of Ag-GO treatment on germination percentage, the lengths of
200   the root and shoot, H_2O_2 content, and Ag content in seedlings. Additionally, one-way ANOVA

201 was conducted to compare the effects of treatments with Ag-GO, Ag NPs, and GO at a
202 concentration of 1.6 mg mL^{-1}. The effects of the treatments were accepted as significant at α =
203 0.05. Tukey's honestly significant difference test was conducted to further investigate which
204 means differed from other means within a group ($p < 0.05$) when the effect of each treatment was
205 significant for the parameters studied. In addition, regression analyses were performed to
206 determine the relationship between the concentration of Ag-GO treatment and Ag content in
207 seedlings treated with Ag-GO.
208

Results

Characterization of Ag-GO

211 The TEM images of Ag-GO showed that the Ag NPs were formed on the wrinkled surface of
212 GO (Figure 1A, B). The average diameter of Ag NPs was 57.5 ± 1.9 (average ± one standard
213 error; $n = 250$) nm. The UV-VIS spectrum of GO (Figure 1C) displayed no obvious absorption
214 band in the wavelength range of 300 to 800 nm. In contrast, the UV-VIS spectrum of Ag-GO
215 showed maximum absorbance at 430 nm, indicating that Ag NPs were loaded on the GO sheets.
216 The Raman spectra of Ag-GO and GO (Figure 1D) showed two peaks, the D band at 1350 cm^{-1}
217 and the G band at 1590 cm^{-1}. However, the intensity of the D and G bands in the Raman
218 spectrum of Ag-GO was enhanced by surface-enhanced Raman scattering. The I_D/I_G ratios of GO
219 and Ag-GO are 0.95 and 0.92, respectively. Analysis of surface bonding using XPS (Figure 1E,
220 F) clearly showed that the intensity of oxygenated carbon bonds decreased after Ag NP
221 formation on GO. The XPS C1s spectra of GO showed three main peaks, for C–C, C–O, and
222 C=O bonds. The C–O and C=O bond peaks of Ag-GO showed a relatively lower intensity than
223 those of GO. Additionally, the carbon-to-oxygen ratio increased from 2.0 to 4.1 after Ag NP
224 formation on the GO sheet. The reduction of oxygenated carbon after Ag NP formation on a GO
225 sheet has also been demonstrated by other groups (Tang et al., 2013; Kim et al., 2018). The
226 weight ratio of Ag to GO was approximately 0.64.
227

Effects of Ag-GO on seed germination and seedling growth

229 Treatment with Ag-GO had no significant effect on germination percentage (Table 1). In
230 addition, germination percentage was not altered by Ag NP or GO treatment. Regardless of the
231 Ag-GO treatment concentration, 100% of the alfalfa and cucumber seeds germinated on day 4
232 and day 7, respectively, and 95-100% of radish seeds germinated on day 7. Ag-GO had both
233 positive and negative effects on seedling growth (Figure 2). The shoot length of alfalfa was not
234 affected significantly by Ag-GO treatment; however, that of radish and cucumber showed a
235 significant response to treatment with Ag-GO (Figure 2A). More specifically, the shoot length of
236 radish treated with Ag-GO at 0.2 to 1.6 mg mL^{-1} increased up to 52% ($p < 0.0001$) and that of
237 radish treated with Ag NPs at 1.6 mg mL^{-1} increased by 36% when compared to the control.
238 However, the shoot length of cucumber decreased by 16% upon treatment with Ag-GO at 0.8 mg
239 mL^{-1} compared to the control ($p = 0.0003$).
240

241   Ag-GO treatment also had a significant effect on the root growth of alfalfa and radish (Figure
242   2B). Treatment with 1.6 mg mL^{-1} of Ag-GO inhibited the root elongation of alfalfa by 41%
243   compared to that of the control ($p = 0.0011$). However, the root length of radish treated with 0.2
244   mg mL^{-1} of Ag-GO increased by 45% compared to that of the control ($p = 0.0456$) and its effect
245   on root elongation significantly differed from that of 1.6 mg mL^{-1} of GO ($p = 0.0002$). In
246   contrast, treatment with Ag-GO had no significant effect on the root length of cucumber.
247   Overall, the effects of Ag-GO, Ag NPs, and GO treatments on root elongation differed
248   significantly ($p < 0.001$).
249
250   **H$_2$O$_2$ content in seedlings treated with Ag-GO**
251   Ag-GO treatment significantly increased the H$_2$O$_2$ content in alfalfa and radish seedlings (Figure
252   3). When alfalfa was treated with 1.6 mg mL^{-1} of Ag-GO, its H$_2$O$_2$ content was more than twice
253   that of the control ($p < 0.0001$) and similar to that in alfalfa treated with 1.6 mg mL^{-1} of Ag NPs
254   ($p < 0.0001$). In radish, the production of H$_2$O$_2$ was increased by treatment with Ag-GO
255   compared to that in the control ($p < 0.0001$). In addition, the level of H$_2$O$_2$ significantly differed
256   for Ag-GO, Ag NPs, and GO treatments ($p < 0.0001$). In contrast, the content of H$_2$O$_2$ in
257   cucumber seedlings was not altered by Ag-GO, Ag NPs, or GO treatments.
258
259   **Ag content of seedlings treated with Ag-GO**
260   The results of the regression analysis showed that the concentration of Ag-GO and the Ag
261   content in the three seedlings were positively correlated. For example, the Ag content in alfalfa
262   was positively correlated with the treatment concentration of Ag-GO ($p < 0.001$, $R^2 = 0.85$).
263   Likewise, in the case of radish and cucumber, there was positive correlation between the
264   concentration of Ag-GO and Ag content in these species ($p = 0.004$, $R^2 = 0.71$ in radish and $p <$
265   0.0001, $R^2 = 0.94$ in cucumber). According to the ANOVA results, there were no significant
266   differences in the Ag content in alfalfa and radish at the concentrations of 0.2, 0.4, and 0.8 mg
267   mL^{-1} of Ag-GO. However, at 1.6 mg mL^{-1} of Ag-GO, Ag accumulation in alfalfa and radish was
268   significantly higher than that for the other treatments ($p < 0.0001$ and $p = 0.0059$, respectively).
269   In cucumber, there was no significant difference in Ag content between 0.2 and 0.4 mg mL^{-1} of
270   Ag-GO treatments, but the Ag content was significantly higher at 0.8 and 1.6 mg mL^{-1} of Ag-GO
271   ($p < 0.001$) (Figure 4). The Ag contents in alfalfa and radish treated with 1.6 mg mL^{-1} of Ag-GO
272   were 93.9 ± 11.6 ng mg^{-1} fresh weight (F.W.), and 43.6 ± 2.0 ng mg^{-1} F.W., respectively. The Ag
273   content in cucumber treated with 1.6 mg mL^{-1} of Ag-GO was 12.5 ± 1.5 ng mg^{-1} F.W., which
274   was four times the content of Ag in cucumber treated with 0.2 mg mL^{-1} of Ag-GO. Furthermore,
275   the Ag content for Ag-GO and Ag NP treatments was significantly different in alfalfa and radish.
276   The Ag content in alfalfa and radish exposed to 1.6 mg mL^{-1} of Ag-GO was approximately two
277   times that of seedlings treated with 1.6 mg mL^{-1} of Ag NPs ($p < 0.0049$ and $p = 0.0079$,
278   respectively). However, the Ag content in cucumber was similar for both treatments (Figure 4).
279
280   **Discussion**

281 The effects of Ag-GO on the early growth of plants were dependent on the plant species with
282 different seed size. The three species used in the present study are from different plant families
283 and have seeds of different sizes, and they showed distinct responses to Ag-GO. Root elongation
284 of the small-seeded alfalfa and radish were enhanced and inhibited, respectively, by Ag-GO
285 treatment, but that of the large-seeded cucumber was not affected. Similarly, in studies that have
286 determined the effects of multi-walled carbon nanotubes, the germination of small-seeded
287 species such as lettuce were affected whereas large-seeded species such as cucumber were not
288 affected by multi-walled carbon nanotube treatment. Therefore, the difference in seed size might
289 be a factor that accounts for the difference in the response of plants to nanomaterials (Cañas et
290 al., 2008; Begum et al., 2012). Additionally, according to previous studies, the effects of
291 nanomaterials on plants depend on the characteristics of the nanomaterials and the xylem
292 anatomy of the plants, which affect the absorption of the nanomaterials onto the root (Cañas et
293 al., 2008; Begum, Ikhtiari & Fugetsu, 2011). Begum, Ikhtiari & Fugetsu (2011) showed that the
294 response of cabbage, tomato, red spinach, and lettuce to graphene depends on the plant species,
295 because of differences in root systems. High concentrations of graphene inhibited the growth of
296 cabbage, tomato, and red spinach, but had no significant effect on lettuce. These results are likely
297 due to the difference in the uptake of nanomaterials by distinctive xylem structures. Likewise,
298 Cañas et al. (2008) reported that the response of plants to nanomaterials varies among plant
299 species and that it depends on the characteristics of nanomaterials.
300
301 In our study, treatment with Ag-GO and Ag NPs increased the length of shoots and roots in
302 radish but had no effect on root length in cucumber. However, in another study, radish and
303 cucumber treated with Ag NPs showed different responses compared to our results, owing to the
304 properties of the nanomaterials used. More specifically, Ag NPs with a size in the range of 1 to
305 10 nm decreased elongation of the shoot and root when applied at a concentration of 0.5 mg mL^{-1}
306 (Zuverza-Mena et al., 2016). Altogether, the responses of the plants vary depending on the
307 characteristics of the nanomaterials, such as the particle size.
308
309 Treatment with Ag-GO led to the production of H_2O_2 during early seedling growth, but relatively
310 low levels of H_2O_2 may enhance seedling growth. Plants produce several kinds of ROS as
311 byproducts of aerobic metabolic pathways, and excessive ROS can cause oxidative damage to
312 proteins, DNA, lipids, and finally cell death (Apel and Hirt, 2004). Several studies demonstrated
313 that nanomaterials produced H_2O_2 and induced oxidative stress in plants (Begum, Ikhtiari &
314 Fugetsu, 2011; Anjum et al., 2013). Begum, Ikhtiari & Fugetsu (2011) showed that graphene
315 induced dose-dependent H_2O_2 accumulation in cabbage, tomato, and red spinach at
316 concentrations of 500, 1000, and 2000 mg L^{-1} using the ROS-sensitive probe 2′,7′-
317 dichlorofluorescein diacetate (DCFH-DA). It induced oxidative stress by causing cell membrane
318 damage and electrolyte leakage in leaves. According to our results, high concentrations of H_2O_2
319 in alfalfa induced by Ag-GO likely inhibited root growth. However, the relatively low levels of
320 H_2O_2 in radish and cucumber weakly affected the seedling growth. In a previous study, Anjum et

321 al. (2013) demonstrated that the activity of catalase and ascorbate peroxidase in faba bean (*Vicia*
322 *faba* L.) seedlings was increased by treatment with 400 and 800 mg L^{-1} of graphene, and this
323 prevents the overproduction of H_2O_2 in faba bean seedlings. Consequently, the low level of H_2O_2
324 accumulated in faba bean seedlings could increase the absorption of liquid by seeds, enhancing
325 the emergence and length of the root.
326

327 Seedlings treated with Ag-GO accumulated more Ag at higher concentrations of Ag-GO.
328 Previous studies have also demonstrated that Ag uptake during seedling growth is dose-
329 dependent, but the amount of Ag uptake is different among plant species, treatment
330 concentrations, and the physicochemical properties of Ag NPs (Geisler-Lee et al., 2013;
331 Zuverza-Mena et al., 2016). Geisler-Lee et al. (2013) demonstrated that in *Arabidopsis thaliana*,
332 Ag NPs having a size of 40 nm translocated from border cells to internal root tissue and vascular
333 tissue and that Ag accumulation was dose-dependent. Likewise, the Ag content in radish
334 seedlings treated with 2-nm Ag NPs was concentration-dependent (Zuverza-Mena et al., 2016).
335 This tendency was also observed in tomatoes and castor seeds treated with Ag NPs, but the
336 accumulated amount differed according to several factors, such as the culture medium, seed size
337 or coat, and physicochemical properties of the nanomaterials (Song et al., 2013; Yasur and Rani,
338 2013). Interestingly, the difference between Ag accumulation in seedlings treated with Ag-GO
339 and those treated with Ag NPs was distinct for small-seeded species. Further study is needed to
340 determine whether Ag accumulation is due to the Ag NPs on the GO sheet or due to Ag$^+$ and to
341 investigate the interaction between Ag-GO and the seedling surface.
342

Conclusions
344 We demonstrate here, that Ag-GO can significantly affect the early growth of plants in a species-
345 specific manner. The shoot growth of cucumber and the root growth of alfalfa was inhibited by
346 Ag-GO treatment, whereas the growth of roots and shoots in radish was enhanced by exposure to
347 Ag-GO. The uptake of Ag from Ag-GO by seedlings was dose-dependent. The production of
348 H_2O_2 increased with the concentration of Ag-GO, and high levels of H_2O_2 may account for the
349 inhibited growth of alfalfa and cucumber seedlings. Further study to investigate other ROS and
350 series of antioxidative mechanisms activated by Ag-GO and long-term experiments employing
351 various plant species are necessary before Ag-GO can be utilized more widely in diverse fields.
352

Acknowledgements
354

References
356 Ahamed M, AlSalhi MS, Siddiqui MKJ. 2010. Silver nanoparticle applications and human
357 health. *Clinica Chimica Acta* 411:1841–1848.
358 Alivisatos P. 2004. The use of nanocrystals in biological detection. *Nature Biotechnology* 22:47-
359 52.

360 Anjum NA, Singh N, Singh MK, Sayeed I, Duarte AC, Pereira E, Ahmad I. 2014. Single-bilayer
361 graphene oxide sheet impacts and underlying potential mechanism assessment in germinating
362 faba bean (*Vicia faba* L.). *Science of Total Environment* 472:834-841.
363 Apel K, Hirt H. 2014. Reactive oxygen species: metabolism, oxidative stress, and signal
364 transduction. *Annual Reviews of Plant Biology* 255:373-399.
365 Bao Q, Zhang D, Qi P. 2011. Synthesis and characterization of silver nanoparticle and graphene
366 oxide nanosheet composites as a bactericidal agent for water disinfection. *Journal of Colloid and*
367 *Interface Science* 360:463-470.
368 Barrena R, Casals E, Colón J, Font X, Sánchez A, Punts V. 2009. Evaluation of the ecotoxicity
369 of model nanoparticles. *Chemosphere* 75:850–857.
370 Begum P, Ikhtiari R, Fugetsu B. 2011. Graphene phytotoxicity in the seedling stage of cabbage,
371 tomato, red spinach, and lettuce. *Carbon* 49:3907-3919.
372 Begum P, Ikhtiari R, Fugetsu B, Matsuoka M, Akasaka T, Watari F. 2012. Phytotoxicity of
373 multi-walled carbon nanotubes assessed by selected plant species in the seedling stage. *Applied*
374 *Surface Science* 262, 120-124.
375 Cañas JE, Long M, Nations S, Vadan R, Dai L, Luo M, Ambikapathi R, Lee EH, Olszyk D.
376 2008. Effects of functionalized and nonfunctionalized single-walled carbon nanotubes on root
377 elongation of select crop species. *Environmental Toxicology and Chemistry* 27:1922-1931.
378 Chen J, Sun L, Cheng Y, Lu Z, Shao K, Li T, Hu C, Han H. 2016. Graphene oxide-silver
379 nanocomposite: novel agricultural antifungal agent against *Fusarium graminearum* for crop
380 disease prevention. *ACS Applied Materials Interfaces* 8:24057-24070.
381 Chung H, Kim MJ, Ko K, Kim JH, Kwon HA, Hong I, Park N, Lee S, Kim W. 2015. Effects of
382 graphene oxides on soil enzyme activity and microbial biomass. *Science of Total Environment*
383 514:307-313.
384 El-Temsah YS, Joner EJ. 2012. Impact of Fe and Ag nanoparticles on seed germination and
385 differences in bioavailability during exposure in aqueous suspension and soil. *Environmental*
386 *Toxicology* 27:42-49.
387 Fleming S, Ulijn RV. 2014. Design of nanostructures based on aromatic peptide amphiphiles.
388 *Chemical Society Reviews* 43:8150-8177.
389 Geisler-Lee J, Wang Q, Yao Y, Zhang W, Geisler M, Li K, Huang Y, Chen Y, Kolmakov A, Ma
390 X. 2013. Phytotoxicity, accumulation and transport of silver nanoparticles by *Arabidopsis*
391 *thaliana*. *Nanotoxicology* 7:323–337.
392 Hummers Jr WS, Offeman RE. 1958. Preparation of graphitic oxide. *Journal of American*
393 *Chemistry Society* 80:1339-1339.
394 Jiao J, Yuan C, Wang J, Xia Z, Xie L, Chen F, Li Z, Xu B. 2016. The role of graphene oxide on
395 tobacco root growth and its preliminary mechanism. *Journal of Nanoscience Nanotechnology*
396 16:12449-12454.
397 Kim MJ, Ko D, Ko K, Kim D, Lee JY, Woo SM, Kim W, Chung H. 2018. Effects of silver-
398 graphene oxide nanocomposites on soil microbial communities. *Journal of Hazardous Materials*
399 346:93-102.

400 Ko K, Yu Y, Kim MJ, Kweon J, Chung H. 2018. Improvement in fouling resistance of silver-
401 graphene oxide coated polyvinylidene fluoride membrane prepared by pressurized filtration.
402 *Separation and Purification Technology* 194:161-169.
403 Li J, Kuang D, Feng Y, Zhang F, Xu Z, Liu M, Wang D. 2013. Green synthesis of silver
404 nanoparticles–graphene oxide nanocomposite and its application in electrochemical sensing of
405 tryptophan. *Biosensors and Bioelectronics* 42, 198-206.
406 Liang Y, Yang D, Cui J. 2017. A graphene oxide/silver nanoparticle composite as a novel
407 agricultural antibacterial agent against *Xanthomonas oryzae* pv. *oryzae* for crop disease
408 management. *New Journal of Chemistry* 41:13692-13699.
409 Migliore L, Cozzolino S, Fiori M. 2003. Phytotoxicity to and uptake of enrofloxacin in crop
410 plants. *Chemosphere* 52:1233–1244.
411 Naeem H, Ajmal M, Qureshi RB, Muntha ST, Farooq M, Siddiq M. 2019. Facile synthesis of
412 graphene oxide–silver nanocomposite for decontamination of water from multiple pollutants by
413 adsorption, catalysis and antibacterial activity. *Journal of Environmental Management* 230:199-
414 211.
415 Nair R, Varghese SH, Nair BG, Maekawa T, Yoshida Y, Kumar DS. 2010. Nanoparticulate
416 material delivery to plants. *Plant Science* 179:154-163.
417 Ocsoy I, Paret ML, Ocsoy MA, Kunwar S, Chen T, You M, Tan W. 2013. Nanotechnology in
418 plant disease management: DNA-directed silver nanoparticles on graphene oxide as an
419 antibacterial against *Xanthomonas perforans*. *ACS Nano* 7:8972-8980.
420 Rui M, Ma C, Tang X, Yang J, Jiang F. Pan Y. Xiang Z, Hao Y, Rui Y, Cao W, Xing B. 2017.
421 Phytotoxicity of silver nanoparticles to peanut (*Arachis hypogaea* L.): physiological responses
422 and food safety. *ACS Sustainable Chemistry and Engineering* 5, 6557-6567.
423 Song B, Zhang C, Zeng G, Gong J, Chang Y, Jiang Y. 2016. Functional analyses of nanoparticle
424 toxicity: a comparative study of the effects of TiO_2 and Ag on tomatoes (*Lycopersicon*
425 *esculentum*). *Ecotoxicology and Environmental Safety* 93:60-67.
426 Tang XZ, Li X, Cao Z, Yang J, Wang H, Pu X, Yu ZZ. 2013. Synthesis of graphene decorated
427 with silver nanoparticles by simultaneous reduction of graphene oxide and silver ions with
428 glucose. *Carbon* 59:93-99.
429 US Environmental Protection Agency. Ecological Effects Test Guidelines OCSPP 850.4150:
430 Vegetative Vigor. Office of Chemical Safety and Pollution Prevention. 2012; Washington, DC
431 Vance ME, Kuiken T, Vejerano EP, McGinnis SP, Hochella Jr, MF, Rejeski D, Hull MS. 2015.
432 Nanotechnology in the real world: Redeveloping the nanomaterial consumer products inventory.
433 *Beilstein Journal of Nanotechnology* 6:1769–1780.
434 Wierzbicka M, Obidzińska J. 1998. The effect of lead on seed imbibition and germination in
435 different plant species. *Plant Science* 137:155–171.
436 Xu WP, Zhang LC, Li JP, Lu Y, Li HH, Ma YN, Wang WD, Yu SH. 2011. Facile synthesis of
437 silver@graphene oxide nanocomposites and their enhanced antibacterial properties. *Journal of*
438 *Materials Chemistry* 21:4593-4597.

439   Yang J, Jiang F, Ma C, Rui Y, Rui M, Adeel M, Cao W, Xing B. 2018. Alteration of crop yield
440   and quality of wheat upon exposure to silver nanoparticles in a life cycle study. *Journal of*
441   *Agricultural and Food Chemistry* 66: 2589-2597.
442   Yang K, Huang LJ, Wang YX, Du YC, Tang JG, Wang Y, Cheng MM, Zhang Y, Kipper MJ,
443   Belfiore LA, Wickramasinghe SR. 2019. Graphene oxide/nanometal composite membranes for
444   nanofiltration: synthesis, mass transport mechanism, and applications. *New Journal of Chemistry*
445   43:2846-2860.
446   Yasur J, Rani PU. 2013. Environmental effects of nanosilver: impact on castor seed germination,
447   seedlings growth, and plant physiology. *Environmental Science and Pollution Research*
448   20:8636–8648.
449   Zhang M, Gao B, Chen J, Li Y. 2015. Effects of graphene on seed germination and seedling
450   growth. *Journal of Nanoparticle Research* 17:1-8.
451   Zhao X, Li N, Jing M, Zhang Y, Wang W, Liu L, Xu Z, Liu L, Li F, Wu N. 2019.
452   Monodispersed and spherical silver nanoparticles/graphene nanocomposites from gamma-ray
453   assisted in-situ synthesis for nitrite electrochemical sensing. *Electrochimica Acta* 295:434-443.
454   Zuverza-Mena N, Armendariz R, Peralta-Videa JR, Gardea-Torresdey JL. 2016 Effects of silver
455   nanoparticles on radish sprouts: root growth reduction and modifications in the nutritional value.
456   *Frontiers in Plant Science* 7:90.

Figure 1

Characterization of Ag–GO and GO.

(A, B) Transmission electron microscope (TEM) images of Ag–GO. (C) Ultraviolet–visible (UV–VIS) spectrum, (D) Raman spectrum, X-ray photoelectron spectroscope (XPS) C1s spectra and binding energy of (E) GO and (F) Ag–GO.
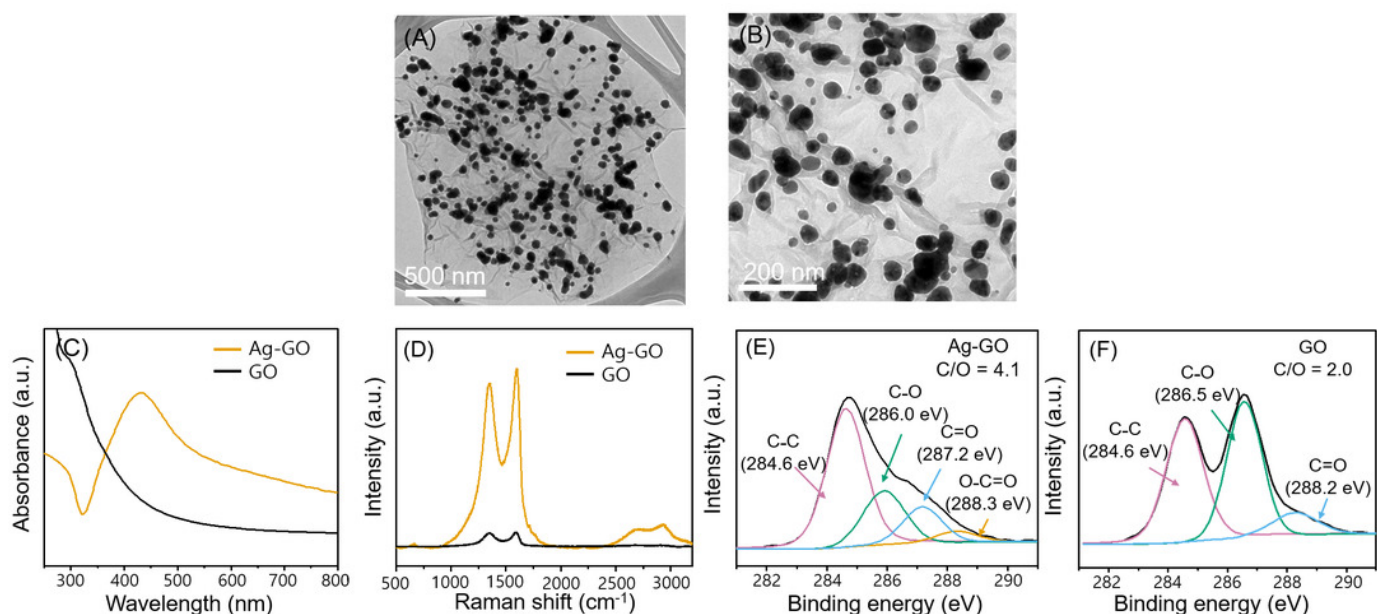
Figure 2

Effects of Ag–GO on the growth of alfalfa, radish, and cucumber seedlings. (A) Shoot length and (B) root length of seedlings at day 7.

Means followed by the same letter are not significantly different at $\alpha = 0.05$. Letters *a* and *b* indicate a significant difference among Ag–GO treatments at different concentrations, and *x*, *y*, and *z* indicate that among 1.6 mg mL^{-1} of Ag–GO, Ag NP, and GO treatments. Error bars represent one standard error ($n = 4$).
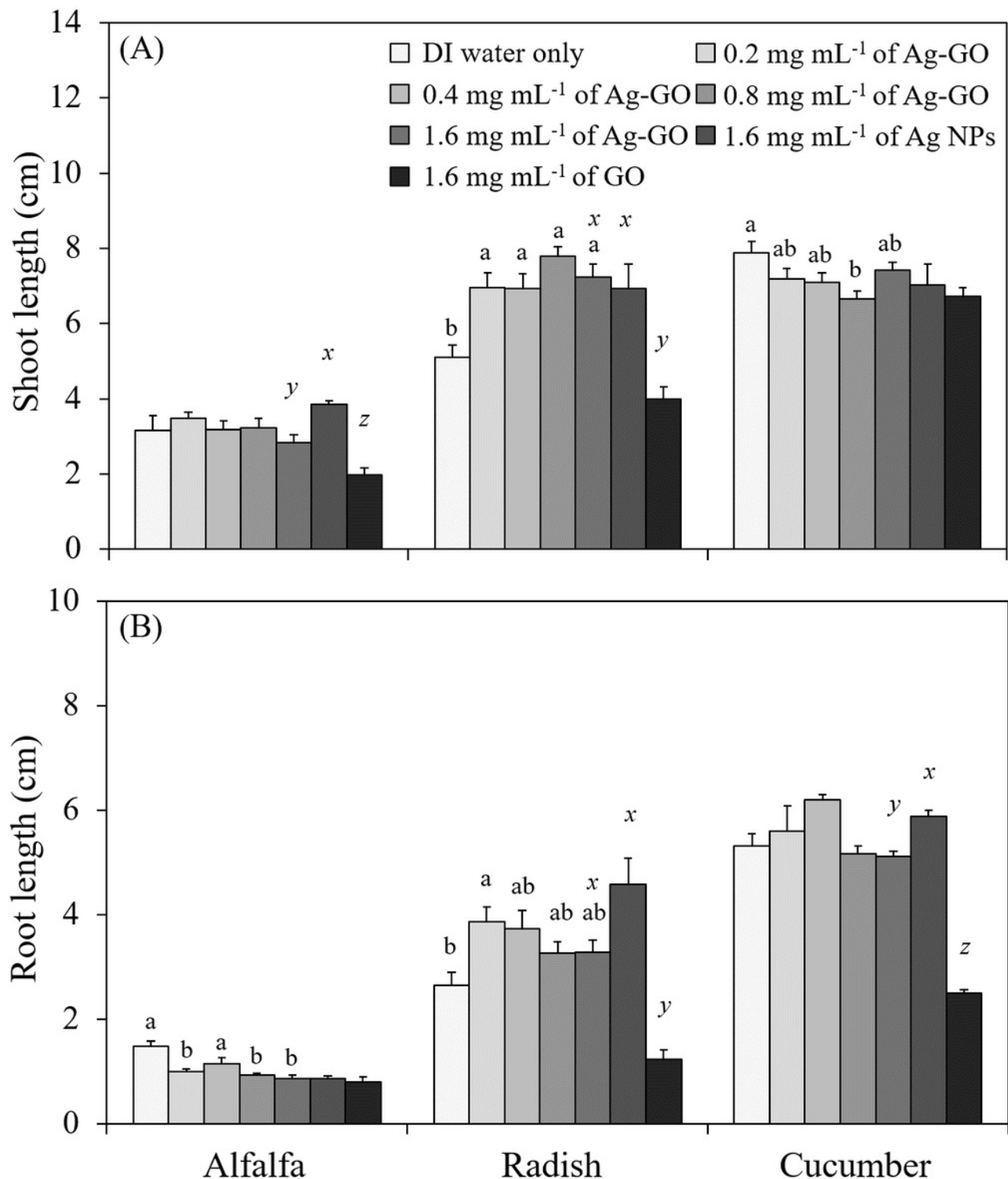
Figure 3

Effects of Ag–GO on the accumulation of H_2O_2 in alfalfa, radish, and cucumber seedlings at day 7.

Means followed by the same letter are not significantly different at $\alpha = 0.05$. Letters *a, b*, and *c* indicate a significant difference among Ag–GO treatments at different concentrations, and *x, y*, and *z* indicate that among 1.6 mg mL^{-1} of Ag–GO, Ag NP, and GO treatments. Error bars represent one standard error ($n = 4$).
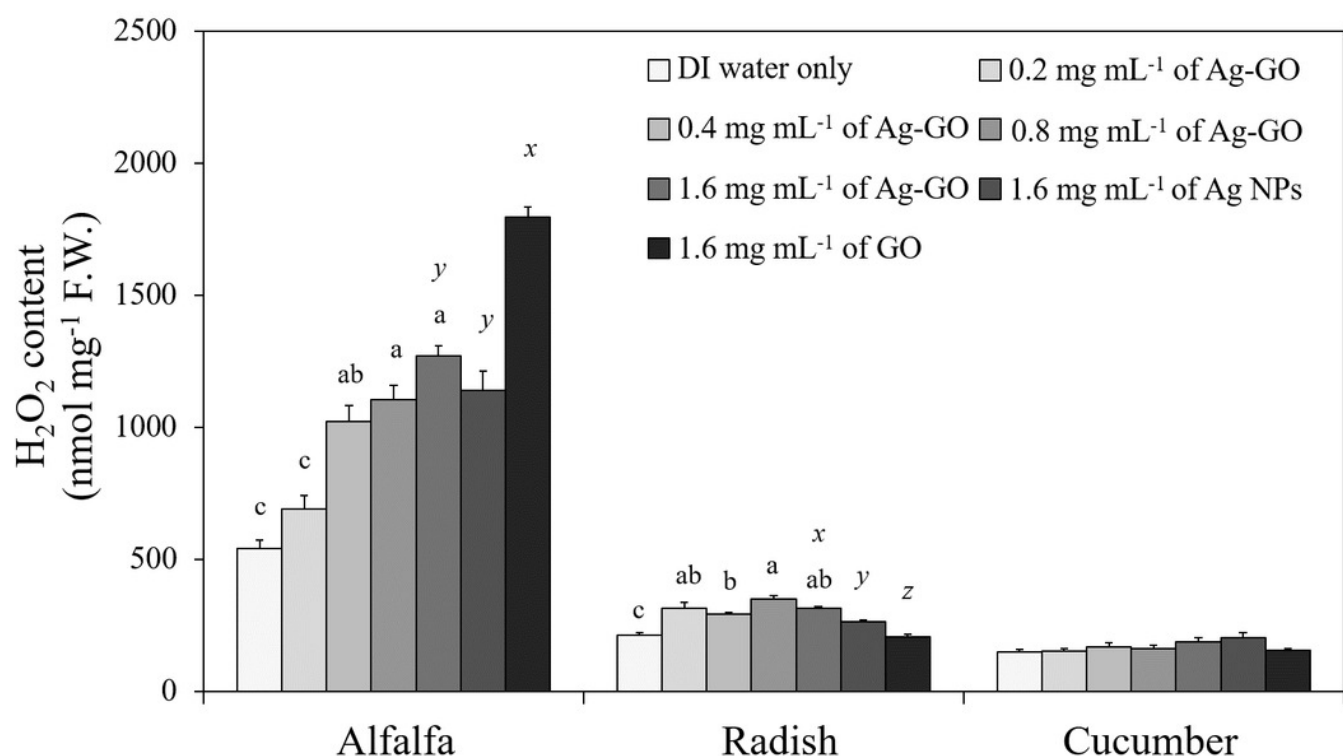
Figure 4

Concentration of Ag in seedlings exposed to Ag–GO at 0.2, 0.4, 0.8, and 1.6 mg mL^{-1} and Ag NPs at 1.6 mg mL^{-1} for seven days (average ± one standard error, n = 4).

The letters a, b, and c denote a significant difference among Ag–GO treatments and x and y denote that between 1.6 mg mL^{-1} of Ag–GO and 1.6 mg mL^{-1} of Ag NP treatments.
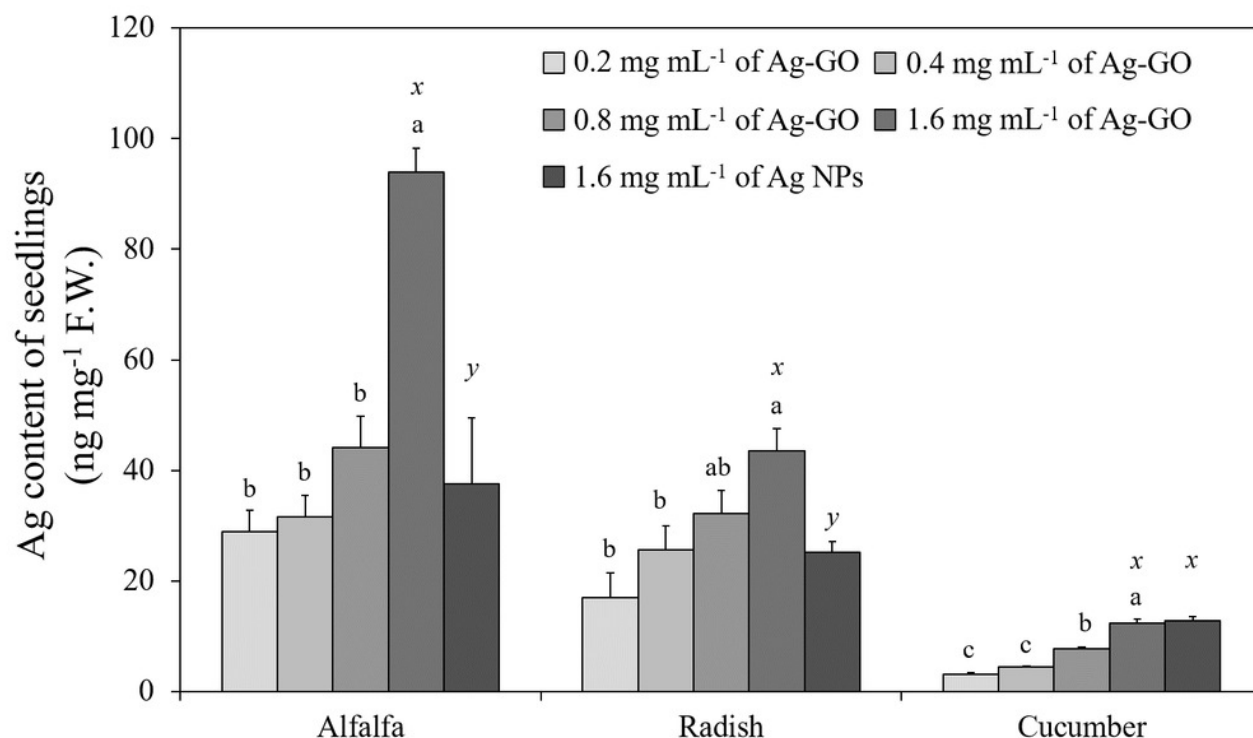
Germination percentage (%) of seedlings treated with Ag–GO, Ag NPs, and GO.

Germination percentage (%) of seedlings treated with Ag–GO, Ag NPs, and GO (average ± one standard error, $n = 4$)

	Alfalfa			Radish			Cucumber		
	Day 2	Day 4	Day 7	Day 2	Day 4	Day 7	Day 2	Day 4	Day 7
DI water only	100	100	100	80 ± 8	93 ± 5	100	100	100	100
0.2 mg/mL of Ag-GO	87 ± 6	100	100	89 ± 4	97 ± 3	100	100	100	100
0.4 mg/mL of Ag-GO	72 ± 12	100	100	91 ± 3	95 ± 4	95 ± 4	96 ±2	100	100
0.8 mg/mL of Ag-GO	87 ± 4	100	100	73 ± 6	90 ± 5	100	100	100	100
1.6 mg/mL of Ag-GO	90 ± 4	100	100	87 ± 6	100	100	100	100	100
1.6 mg/mL of Ag NPs	90 ± 4	100	100	87 ± 5	97 ± 3	100	100	100	100
1.6 mg/mL of GO	100	100	100	100	100	100	100	100	100